Journal of Physics:
Conference Series

PAPER • OPEN ACCESS

Towards dynamic urban environmental exposure assessments: a case study of the Brussels Capital Region

To cite this article: YS Huang *et al* 2025 *J. Phys.: Conf. Ser.* **3140** 122002

Journal of Physics: Conference Series **3140** (2025) 122002 doi:10.1088/1742-6596/3140/12/122002

Towards dynamic urban environmental exposure assessments: a case study of the Brussels Capital Region

YS Huang[1], M Llaguno-Munitxa[1,2] and G Manoli[3]

[1]LAB, UCLouvain, Louvain-la-Neuve, Belgium
[2]LOCI, UCLouvain, Tournai, Belgium
[3]ENAC IA URBES, EPFL, Lausanne, Switzerland

E-mail: `yen-shuo.huang@uclouvain.be`, `maider.llaguno@uclouvain.be`, `gabriele.manoli@epfl.ch`

Abstract. This study proposes a multi-dimensional *dynamic exposure assessment* methodology for outdoor environments, which incorporates factors such as heat, cold, air pollution, sky view factor, and greenery, along with population dynamics. Utilizing high spatiotemporal resolution data, the dynamic exposure assessment captures temporal and spatial variations in urban environmental exposures and evaluates the effectiveness of green infrastructure and urban planning features in mitigating environmental stressors. This approach offers novel insights compared to conventional *static exposure assessments*, which rely on fixed census-based population data and overlook diurnal and seasonal variability. Focusing on the Brussels Capital Region (BCR), the study analyzed exposure during the two hottest days and the annual average for the year 2011. The indicators of Mean Radiant Temperature (Tmrt) and Universal Thermal Comfort Index (UTCI) for day and night were computed for all soft mobility routes — non-motorized urban pathways used by pedestrians, cyclists, e-scooter users, etc — located in the BCR. For the hottest days, the results showed that ∽60% and ∽40% of the soft mobility routes are exposed to moderate (26 to 32 °C UTCI) and strong heat stress (above 32 °C UTCI), respectively. For the annual average, we calculated the difference between the dynamic and static exposure assessment methods. The results indicate that the static method underestimates heat exposure by ∽51%, cold exposure by ∽10%, and air pollution and greenery exposure by ∽8%. These findings support urban design policies by highlighting soft mobility routes that need strategic planning to reduce exposure risks.

1. Introduction

Urban residents are more exposed to environmental stressors than their rural counterparts, with these exposures expected to increase due to climate change [1–4]. Government sectors and urban planners struggle to mitigate these hazards or pinpoint problematic urban areas due to limitations in previous studies and the lack of standardized frameworks [5]. Research has examined both negative (e.g., heat, air pollution) and positive (e.g., greenery) exposures, yet multidimensional assessments remain limited, and they typically rely on static population data failing to consider the exposure variability driven by population dynamics [6–10].

Furthermore, most of these studies focus on the city scale [7, 9], treating urban areas as homogeneous and thereby overlooking exposure pathways. For example, these studies do not account for the different exposures to greenery in the urban spaces or the duration spent by different population subgroups in distinct areas [6, 10]. Additionally, population dynamics are often ignored [8].

Over the past decade, dynamic air pollution assessments have utilized mobile phone data [11, 12] and time-use surveys [13] to bridge the gap between individual-level studies with wearable sensors and city/regional-level analyses with census data. In contrast, dynamic heat exposure studies face several unresolved issues [14–16]. These studies often rely on incomplete meteorological data, such as regulatory station daily mean air temperatures [14], or coarse spatial and temporal resolution surface [15] and near-surface temperatures [16]. Furthermore, while previous studies identify links between population and Urban Heat Island (UHI) intensity [17] and the independent mortality effects of air pollution and noise [18], most exposure assessments neglect environmental synergies [19]. This oversight risks misattribution in exposure evaluations [20].

That is, most existing studies have: (i) overlooked population dynamics despite known urban activity variations and significant day/night population fluctuations, (ii) oversimplified exposure pathways and misjudged exposure duration and location, (iii) generally relied on temperature as thermal comfort indicator due to limited urban environmental data, and (iv) assessed exposures separately, often neglecting comprehensive evaluations of multiple stressors and synergistic effects.

To address these challenges, this research proposes a multidimensional environmental exposure assessment methodology that accounts for dynamic population data considering day and night variations. Focusing on the BCR, the study analyzed exposure during the two hottest days and the annual average for the year 2011.

2. Methodology

2.1. Data

Figure 1 provides an overview of the data. We utilized day/night population data at a 1km $\times$ 1km resolution, integrating statistics from the 2011 European Census and geospatial data [21] made available in the BCR. Socio-economic data were also incorporated, in line with previous studies indicating that environmental stressors, such as air pollution, may be associated with socioeconomic status [22–24](see report by CurieuzenAir 2021 citizen science project in BCR where areas with lower car ownership were said to experience poorer air quality [23]). Hence, we included data from the Belgium Index of Multiple Deprivation (BIMD) [25], which encompasses six domains: income, employment, education, housing, crime, and health.

Meteorological data were sourced from hourly climate simulations of the UrbClim model [26] with an initial resolution of 100m $\times$ 100m, upscaled by the factor of 10 to be spatially consistent with population data, and providing 2011 metrics for ambient temperature, relative humidity, and wind speed. These were combined with solar radiation data [27] to compute Tmrt and UTCI. Air pollution data, including monthly NO_2, $PM_{2.5}$, PM_{10}, and O_3 concentrations at a 100m $\times$ 100m resolution, were processed using geographically weighted regression (GWR) and random forest (RF) models [28].

Urban greenery was represented using the 16-day Normalized Difference Vegetation Index (NDVI) at a 250m $\times$ 250m resolution [29]. The detailed urban fabric included the Sky View Factor (SVF) at 2m $\times$ 2m resolution, and land use at 10m $\times$ 10m resolution, both processed from the Digital Terrain Model (DTM) from 2021 [30], the Digital Surface Model (DSM) from 2021 [31], building parcels from 2024 [32], the Corine Land Cover 2012 [33], building volume from 2010 [34], and bike routes from 2024 [35]. All environmental factors were disaggregated to soft mobility route segments, defined by 7-meter buffer zones on each side of the bike routes, with an average segment length of 50 meters (see Figure 2).

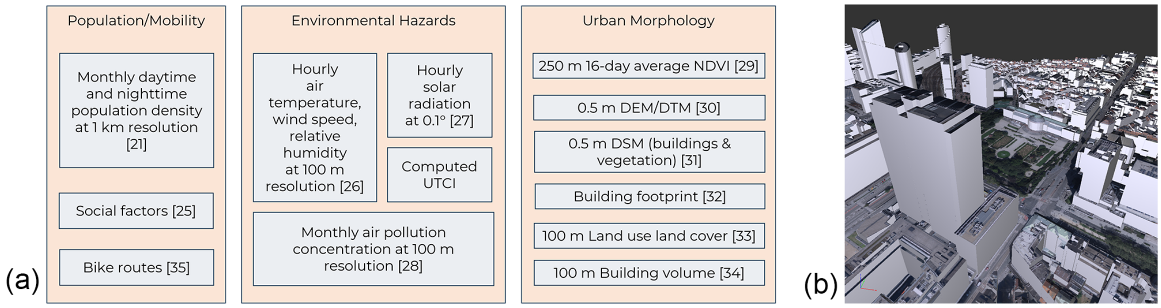

Figure 1. Overview of the data in (a) list and (b) 3D city model.

2.2. Computing UTCI

Day (8 am to 4 pm) and night (4 pm to 12 am) Tmrt and UTCI for each 1km × 1km grid were calculated using the QGIS plugin UMEP-SOLWEIG [36] and the Python package pythermalcomfort [37], as illustrated in Figure 2. The final spatial resolution is determined by the input DSM. The original 0.5m DSM proved impractical due to excessive computational demands. After a sensitivity check, a 2m UTCI resolution was chosen, balancing efficiency and accuracy.

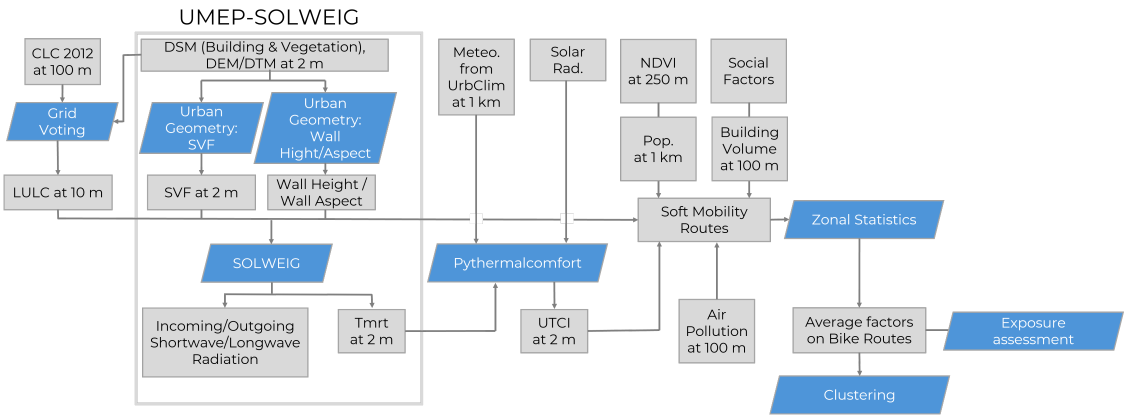

Figure 2. Procedures of the proposed method.

2.3. Exposure assessment

Dynamic environmental factors were linked to the day/night populations for the exposure assessment. The dynamic population is assumed to be evenly distributed along the soft mobility routes, normalized by the segment area. The exposure assessment for the soft mobility routes was computed for two hottest days and year average for 2011.

The hottest two days of the year 2011 (June 27 and 28) were selected to analyze the correlation between environmental/social factors and urban canyon quality under extreme conditions. Soft mobility route segments were clustered based on environmental factors to identify urban infrastructures needing improvement. Clustering was performed using the k-means method [38], with the number of clusters determined by minimizing the squared error and using silhouette scores [39]. These procedures were conducted in QGIS and Python.

For the yearlong study, the definition of the exposure was computed as described in the IPCC AR5 report[40], while heat stress and cold stress are defined as the UTCI above and below the "no thermal stress" level (9 to 26 °C UTCI) [41]. "Degree days" is calculated as the absolute residual between the reference temperature and daily average temperatures, indicating the degree of thermal satisfaction [42, 43]. The heat and cold stress are defined as the monthly cumulative heat and cold degree-hour in Equation 1, where n is the number of days in the month, T_i is the UTCI of each time step, and 8 is the number of hours in a time step. The dynamic method in Equation 2 was applied throughout 2011 to compute the monthly temperature-related exposure at a diurnal resolution. The static method in Equation 3 assumes exposure to the daily average UTCI, leading to significant bias and incomparability with the dynamic method. Both methods excluded the time period between midnight and 8 am, and daily heat and cold exposures are then accumulated into monthly and annual exposures.

$$\mathrm{Stress}_m = 16\sum_{d=1}^{n}\mathrm{Stress}_d = 8\sum_{d=1}^{n}(\mathrm{Stress}_{\textit{8-16, d}} + \mathrm{Stress}_{\textit{16-24, d}}) = 8\sum_{i=1}^{2n}|\mathrm{T}_i - \mathrm{T}_{\textit{ref.}}| \tag{1}$$

$$\mathrm{Exp}_{\textit{dynamic, m}} = 8\sum_{d=1}^{n}\mathrm{Stress}_{\textit{8-16, d}}\times\mathrm{Pop}_{\textit{day, m}} + 8\sum_{d=1}^{n}\mathrm{Stress}_{\textit{16-24, d}}\times\mathrm{Pop}_{\textit{night, m}} \tag{2}$$

$$\mathrm{Exp}_{\textit{static, m}} = 16\sum_{d=1}^{n}\mathrm{Stress}_d\times\mathrm{Pop}_{\textit{static}} \tag{3}$$

Where $\mathrm{Stress}_{\textit{8-16, d}}$ and $\mathrm{Stress}_{\textit{16-24, d}}$ are day and night outdoor heat/cold stress of each day, $\mathrm{Pop}_{\textit{day, m}}$ and $\mathrm{Pop}_{\textit{night, m}}$ are day/night population of each month, and $\mathrm{Pop}_{\textit{static}}$ is the annual average nighttime population density.

We utilized the monthly air pollution concentration to compare exposure assessments at different temporal resolutions and with or without mobility, as shown in Equations 4 and 5 where C_m and $\mathrm{C}_{\textit{annual}}$ are the monthly and annual average air pollutant concentrations. Greenery exposure uses the same equations as air pollution, simply replacing C_m with NDVI_m.

$$\mathrm{Exp}_{\textit{dynamic, annual}} = \sum_{m=1}^{12}\mathrm{Exp}_m = \sum_{m=1}^{12}\mathrm{C}_m\times\frac{\mathrm{Pop}_{\textit{day, m}} + \mathrm{Pop}_{\textit{night, m}}}{2} \tag{4}$$

$$\mathrm{Exp}_{\textit{static, annual}} = \mathrm{C}_{\textit{annual}}\times\mathrm{Pop}_{\textit{static}}\times 12 \tag{5}$$

3. Results and Discussion

3.1. Hot days in 2011

Nine clusters were identified for the soft mobility route segment. As shown in Figure 3, clusters 2 and 7 experience high daytime heat exposure, while cluster 8 suffers from poor air quality. Generally, clusters 2 and 8 comprise plazas and boulevards. Conversely, cluster 7 includes typical streets, which would not have been identified as problematic without the proposed method. In these two days, 62.6% and 37.4% of the soft mobility routes are exposed to moderate and strong heat stress (UTCI 26 to 32 °C, 32 to 38 °C), respectively. Figure 4 (a) indicates the strong correlation between heat stress and the absence of greenery, while NO_2 and PM_{10} show higher relationship with social factors. Worse air quality tends to happen in districts with less deprivation in education and income, less greenery and higher building volume.

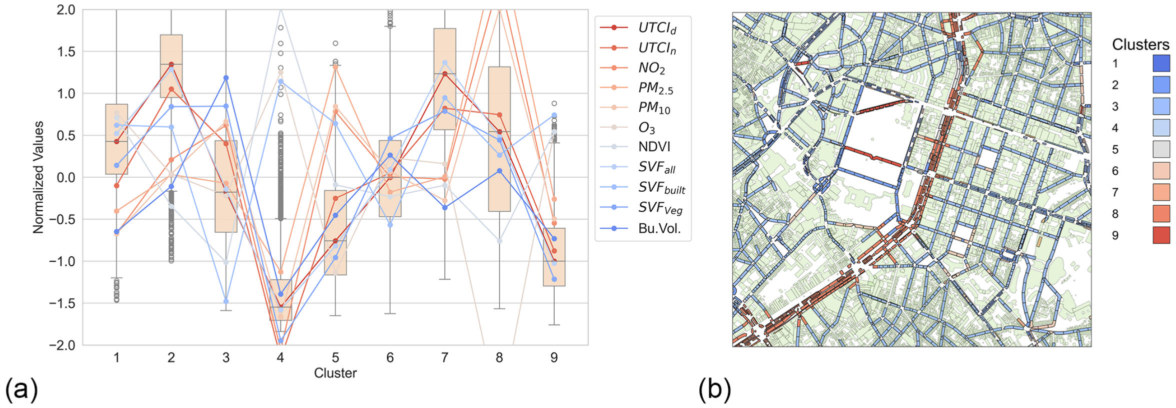

Figure 3. The soft mobility route clusters of the short-term case shown (a) with the factors of each cluster and (b) on a map. Where $UTCI_d$ and $UTCI_n$ are the day/night UTCI, Pop_d and Pop_n are the day/night population, $PM_{2.5}$ and PM_{10} are particle matters, NO_2: nitrogen dioxide, BIMD is the overall score of social deprivation, including crime, education, employment, health, housing, and income. SVF_{all}, SVF_{built}, and SVF_{Veg} are overall SVF, SVF of built-up, and SVF of greenery. The higher SVF indicates lower existence of built-up or greenery. Bu. Vol.: building volume.

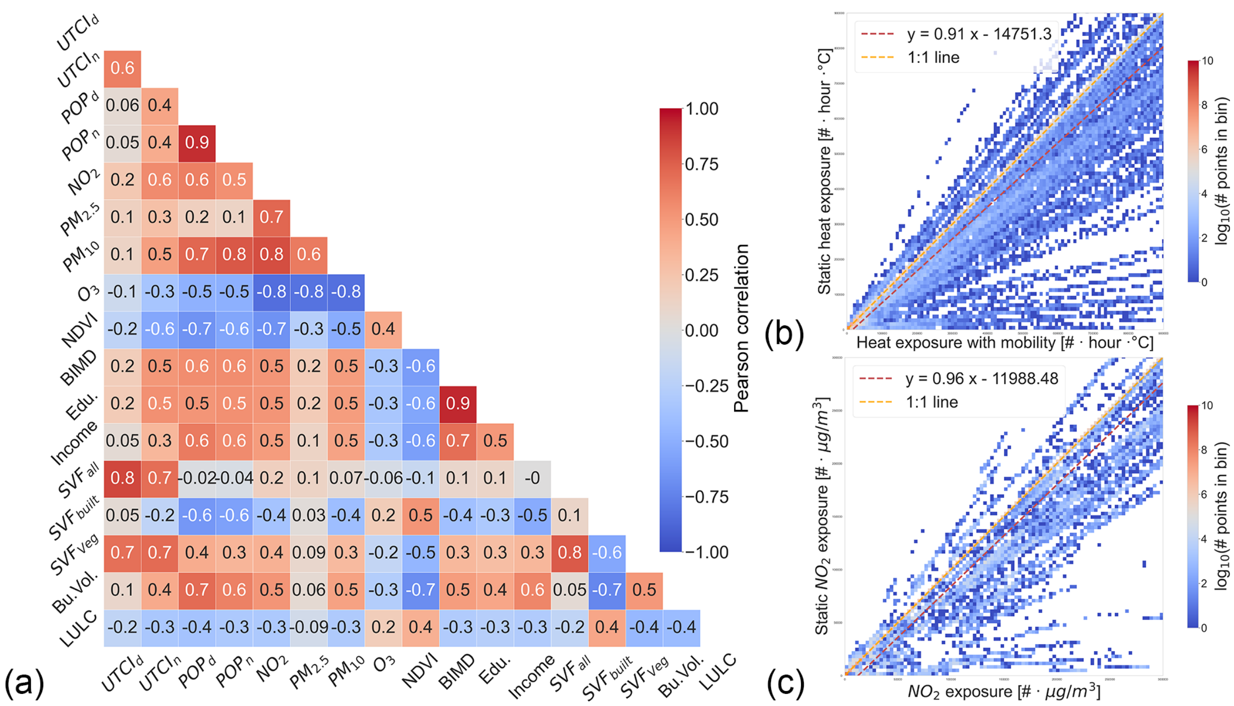

Figure 4. (a) The Pearson correlation between dynamic population, environmental hazards, and urban morphology of the short-term case. Where LULC: land use land cover, and other abbreviations are explained in Figure 3. Density heatmaps of (b) monthly heat exposure in June and (c) monthly NO_2 exposure in June.

Table 1. Percentage of difference between static method and dynamic method. Calculated by normalizing the difference between methods using the results of the dynamic method.

	Population	**Heat stress**	**Cold stress**	**NO_2**	**$PM_{2.5}$**	**PM_{10}**	**O_3**	**NDVI**
Diff.	-15.4%	-51.0%	-9.6%	-7.5%	-7.8%	-7.7%	-7.8%	-7.8%

3.2. Annual dynamic exposure assessment for 2011

Comparing exposure assessments with and without population dynamics revealed that the static method underestimate exposures by over 7%, as shown in Table 1. The error in heat stress is particularly significant, reaching 50.7%, due to the urban temperature amplification by population [17]. Ignoring over 20% more people in urban areas during the day and using daily average meteorological data, static methods miss substantial heat exposures. While greenery exposure shows a 7.6% underestimation due to mobility and air pollution exposures are at the same scale, the synergistic effects between air pollution and population density are not assured. Figure 4 (b) (c) illustrate the exposure difference between the static method and the dynamic method in June, indicating significant differences in considering time and population dynamics. Districts with less deprivation in income and education have high building volume and low greenery cover, which may indicate a lower degree of suburbanization in BCR.

4. Conclusion

Traditional assessments significantly underestimate annual heat exposure by approximately 51% in BCR, a primarily working city with minimal seasonal fluctuations. Air pollution assessments that ignore population dynamics underestimate exposures by about 8%, similar to greenery exposure. Traditional models using low temporal resolution data and static populations overlook transient population surges, potentially underestimating public health impacts. Our approach reveals that urban design features such as plazas and boulevards can exacerbate heat exposure, while some urban areas while including a green canopy may still pose problems. Identifying these factors is crucial for informed urban planning and effective environmental stress mitigation.

Acknowledgments

This work was supported by the Fonds de la Recherche Scientifique-FNRS under Grant T.0137.23.

References

[1] Lüthi, S. et al. 2023. *Nat. Comm.* vol. **14**. 1. pp. 4894.
[2] Vicedo-Cabrera, A. M. et al. 2021. *Nat. Clim. Chan.* vol. **11**. 6. pp. 492–500.
[3] Tran, H. M. et al. 2021. *Sci. of The Tot. Env.* vol. **898**. pp. 492–500.
[4] Kaur, R. and Pandey, P. 2021. *Fron. in Sus. Cit.* vol. **3**. pp. 705131.
[5] He, B.-J. et al. 2023. *Energy and Buildings* vol. **287**. pp. 112976.
[6] Barboza, E. P. et al. 2021. *The Lancet Plan. Hea.* vol. **5**. 10. pp. e718–e730.
[7] Gasparrini, A. et al. 2015. *The Lancet* vol. **386**. 9991. pp. 369–375.
[8] Iungman, T. et al. 2023. *The Lancet* vol. **401**. 10376. pp. 577–589.
[9] Masselot, P. et al. 2021. *The Lancet Plan. He.* vol. **7**. 4. pp. e271–e281.
[10] Rojas-Rueda, D. et al. 2019. *The Lancet Plan. He.* vol. **3**. 11. pp. e469–e477.

[11] Nyhan, M. et al. 2016. *Env. Sci. Tech.* vol. **50**. 17. pp. 9671–9681.
[12] Nyhan, M. et al. 2019. *J. of Exp. Sci. Env. Epid.* vol. **29**. 2. pp. 238–247.
[13] Smith, J. D. et al. 2016. *Env. Sci. Tech.* vol. **50**. 21. pp. 11760–11768.
[14] Yang, J., Hu, L., and Wang, C. 2019. *Sci. Adv.* vol. **5**. 12. pp. eaay3452.
[15] Huang, X., Jiang, Y., and Mostafavi, A. 2024. *npj Urb. Sus.* vol. **4**. 1. pp. 6.
[16] Hu, L., Wilhelmi, O. V., and Uejio, C. 2016. *Sci. of the tot. Env.* vol. **655**. pp. 1–12.
[17] Manoli, G. et al. 2019. *Nat.* vol. **573**. 7772. pp. 55–60.
[18] Tétreault, L.-F., Perron, S., and Smargiassi, A. 2013. *Int. J. of Pub. He.* vol. **58**. pp. 649–666.
[19] Mueller, N. et al. 2017. *Env. He. Persp.* vol. **125**. 1. pp. 89–96.
[20] Vandeninden, B. et al. 2024. *BMC Pub. He.* vol. **24**. 1. pp. 536.
[21] Silva, F. Batista e et al. 2020. *Nat. Comm.* vol. **11**. 1. pp. 4631.
[22] Liu, J. et al. 2021. *Env. He. Persp.* vol. **129**. 12. pp. 127005.
[23] Lauriks, F., Jacobs, D., and Meysman, F. J. 2022 vol. pp. 50.
[24] Josey, K. P. et al. 2023. *New Eng. J. of Med.* vol. **388**. 15. pp. 1396–1404.
[25] Otavova, M. et al. 2023. *Sp. and Spatio-temporal Epid.* vol. **45**. pp. 100587.
[26] Hooyberghs, H. et al. Climate variables for cities in Europe from 2008 to 2017.
[27] CAMS. CAMS gridded solar radiation.
[28] Shen, Y. et al. 2022. *Env. Int.* vol. **168**. pp. 107485.
[29] Didan, K. MOD13Q1 MODIS/Terra vegetation indices 16-day L3 global 250m SIN grid V061.
[30] Paradigm. Digital terrain model - 2021.
[31] Paradigm. UrbIS - Digital surface model.
[32] Paradigm. UrbIS - Parcels and buildings.
[33] EEA. CORINE Land Cover 2012 (raster 100 m), Europe, 6-yearly - version 2020_20u1.
[34] Pesaresi, M. and Politis, P. GHS-BUILT-V R2023A - GHS built-up volume grids (1975-2030).
[35] Paradigm. Geographic Information System Mobility (MOBGIS).
[36] Mutani, G. and Beltramino, S. 2022. *Int. J. of Heat and Tech.* vol. **40**. 4. pp. 871–878.
[37] Tartarini, F. and Schiavon, S. 2020. *SoftwareX* vol. **12**. pp. 100578.
[38] MacQueen, J. 1967. *Proc. of the Fifth Berkeley Sym. on Math. Stat. and Prob., Volume 1: Statistics* vol. **5**. pp. 281–298.
[39] Rousseeuw, P. J. 1987. *J. of Comp. and App. Math.* vol. **20**. pp. 53–65.
[40] Pachauri, R. K. et al. 2014. *IPCC* vol. pp.
[41] Bröde, P. et al. 2012. *Int. J. Biometeorol* vol. **56**. pp. 481–494.
[42] De Rosa, M. et al. 2014. *Applied energy* vol. **128**. pp. 217–229.
[43] Oh, J. W. et al. 2020. *Scientific reports* vol. **10**. 1. pp. 3559.